Stretched states in ^{12,13}B with the (d,α) reaction

A. H. Wuosmaa, J. P. Schiffer, S. Bedoor, M. Albers, M. Alcorta, S. Almaraz-Calderon, B. B. Back, P. F. Bertone, C. M. Deibel, C. R. Hoffman, J. C. Lighthall, S. T. Marley, R. C. Pardo, K. E. Rehm, and D. V. Shetty

Phys. Rev. C **90**, 061301 — Published 8 December 2014

DOI: 10.1103/PhysRevC.90.061301

Stretched states in ^{12,13}B with the (d,α) reaction

A. H. Wuosmaa,[1,2] J. P. Schiffer,[3] S. Bedoor,[1] M. Albers,[3] M. Alcorta,[3,*] S. Almaraz-Calderon,[3] B. B. Back,[3] P. F. Bertone,[3,†] C. M. Deibel,[4] C. R. Hoffman,[3] J. C. Lighthall,[1,*] S. T. Marley,[1,3,‡] R. C. Pardo,[3] K. E. Rehm,[3] and D. V. Shetty[1,§]

[1] *Department of Physics, Western Michigan University, Kalamazoo, Michigan 49008-5252, USA*
[2] *Department of Physics, University of Connecticut, Storrs, Connecticut 06269-3046, USA*
[3] *Physics Division, Argonne National Laboratory, Argonne, Illinois 60439, USA*
[4] *Department of Physics and Astronomy, Louisiana State University, Baton Rouge, Louisiana 70803, USA*

The (d,α) reaction is highly selective, favoring final states in which the removed neutron and proton are completely aligned in a $J = 2j$ configuration. We have studied the ^{14,15}C$(d,\alpha)^{12,13}$B reactions in inverse kinematics using HELIOS at Argonne National Laboratory. In ^{12}B, the reaction strongly favors the population of a known 3^+ state at 5.61 MeV, and for ^{13}B, we observe a possible unreported doublet of states at high excitation energy, probably corresponding to the ^{12}B(3^+) state coupled to the $1s_{1/2}$ neutron from the ^{15}C ground state. In contrast to single-nucleon transfer, deuteron-transfer reactions have not been widely studied with exotic nuclei.

PACS numbers: 21.10.-k, 25.40.Hi, 25.60.Je
Keywords: Transfer reactions, Aligned Configurations, Unstable beams

It has been known for many years that the (d,α) and (α,d) reactions are highly selective [1–6]. This selectivity emerges from a combination of nuclear structure and kinematic considerations and favors the removal or addition of two nucleons in the same shell-model orbit with their angular momenta completely aligned in the $J{=}2j$ state. Unlike the $(p,^3He)$ or $(^3He,p)$ process, where the transferred proton-neutron pair can be either $S{=}0$ or 1, in the (d,α) or (α,d) process the pair *must* be deuteron-like, coupled to $S{=}1$ and $T{=}0$. Such transitions may be approximated as a single-step transfer of a deuteron and the relatively high values of ℓ also tend to be favored by the momentum mismatch between the alpha particle and deuteron. The systematic enhancement of such transitions emerges naturally from the treatment of two-nucleon transfer amplitudes presented by Glendenning [7, 8], as well as from coefficients of fractional parentage for two-nucleon transfer as described, e.g., by Cohen and Kurath [9]. This enhancement was used in the study of high-spin states with the (α,d) reaction, where a large momentum transfer also favors transitions to states with large J and "stretched" nuclear configurations. For example, Rivet *et al.* [2] and Lu *et al.* [3] made assignments for $(0d^2_{5/2})_{5^+}$ and $(0f^2_{7/2})_{7^+}$ states in nuclei from ^{14}N to ^{42}Sc populated in the (α,d) reaction, clearly demonstrating this effect. In the p shell, Van der Woude and de Meijer compared (d,α) and (α,d) reactions on ^{12}C, ^{14}N, and ^{16}O targets, identifying candidates for aligned $(0p_{3/2})^{-2}$ and $(0p_{3/2})^2$ configurations in the residual nuclei [6].

While extremely useful, these properties of deuteron-transfer reactions have not yet been utilized with the more exotic nuclei accessible with rare-isotope beams. Aligned configurations of proton-neutron or proton-neutron-hole pairs are even more interesting when there exists a large imbalance between N and Z. In nuclei near stability, the proton and neutron Fermi surfaces are close to each other, and the aligned states may be at rather low excitation energy. If $N > Z$ then the neutron may be more deeply bound while the proton is at the Fermi surface, and the corresponding state may appear at significantly higher excitation energy, though the reaction Q values for the stretched excitations for $N > Z$ may be more similar to those for $N \approx Z$. Even if the state is well above the neutron-decay threshold, it may remain relatively narrow due to the small overlap between its wave function and a final state that has appreciable proton $p_{3/2}$ hole excitations. The excitations for which deuteron transfer is selective may be inaccessible to the single-nucleon transfer reactions that have been the focus of much recent work done with exotic nuclei.

Here we present new data on the ^{14,15}C$(d,\alpha)^{12,13}$B reactions studied in inverse kinematics using the HELIcal Orbit Spectrometer (HELIOS) [10, 11] at the ATLAS accelerator facility at Argonne National Laboratory. In ^{12}B, the data reveal the strong population of a known state formed from an aligned configuration of $0p_{3/2}$ proton and neutron holes with spins coupled to $J^\pi = 3^+$. In the less-understood ^{13}B nucleus, we observe a pronounced structure that could correspond to a doublet of states at high excitation energy whose neutron configuration likely corresponds to the 3^+ state in ^{12}B coupled to the valence $1s_{1/2}$ neutron from the ground state of ^{15}C.

The measurement was done using ^{14,15}C beams from the ATLAS accelerator at Argonne National Laboratory at energies of 17.1 and 15.7 MeV/nucleon, respectively . The ^{14}C beam was produced directly using enriched ma-

* Present address: TRIUMF, Vancouver, BC V6T 2A3, Canada
† Present address: Marshall Space Flight Center, Huntsville, AL 35811, USA
‡ Present address: University of Notre Dame, South Bend, IN 46558, USA
§ Present address: Grand Valley State University, Allendale, Michigan 49401, USA

terial in a negative-ion sputter source. The ^{15}C beam was produced using the ATLAS In-Flight production facility [12, 13] with the ^{2}H(^{14}C,^{15}C)p reaction, where an intense ($\approx 50-100$ pnA) ^{14}C primary beam bombarded a cryogenic deuterium gas cell. For the measurements with ^{14}C, the beam passed through the gas cell and was limited to an intensity of between 10^7 and 10^8 particles per second on target. The peak intensity of the secondary ^{15}C beam was approximately 5×10^5 particles per second on target, as measured using a silicon surface-barrier telescope placed on the axis of the HELIOS device. For the ^{14}C-beam measurements, the rate in the zero-degree counter was limited by a fine tantalum mesh which attenuated the count rate to a manageable level but made the absolute measurement of the ^{14}C intensity unreliable. The beams passed through a collimation tube with a 5×5 mm^2 square collimator at the end, before reaching the target. The targets consisted of deuterated polyethelene foils $(CD_2)_n$ of areal density 145 μg/cm^2, as well as Au foils for recoil detector calibration, and natural C targets to evaluate the backgrounds produced by interactions of the beam with the carbon in the $(CD_2)_n$.

In HELIOS, light-charged particles are transported in helical orbits from the target to an array of position-sensitive silicon detectors surrounding the beam axis by a uniform magnetic field oriented parallel to the beam direction. Prior measurements with HELIOS [11, 14–17] on (d,p) reactions utilized a configuration where the protons were detected at backward laboratory angles. For the measurements described here the α-particles of interest are emitted at forward angles in the center of mass system and also travel forward in the laboratory. The magnetic field strength was 2.5 T. The silicon-detector array was positioned in the forward hemisphere, covering distances between 942 to 1292 mm downstream of the target. With this experimental arrangement, both ^{3}He and ^{4}He ions were transported to the silicon-detector array; results for the (d,^{3}He) reaction will be presented elsewhere. The silicon-detector array was calibrated using data from a mixed ^{146}Gd-^{248}Cm alpha source, as well as data for known transitions in the (d,^{3,4}He) reactions with the ^{14}C beam.

To detect and identify the recoiling boron ions, a set of silicon-detector telescopes similar to those used in [14–17] was placed on the solenoid axis between the target and the light-charged-particle detector array. The recoil telescopes subtended laboratory polar angles between 1.0 and 5.6 degrees, and 92% of the azimuthal angle range. The detector geometry and magnetic field were chosen so that the alpha particles go around the telescope, and be detected in the HELIOS silicon-detector array. The maximum excursion of the alpha-particle orbits was limited to 25 cm from the solenoid axis by a ring that supported the recoil detector array. The energy-loss and residual-energy resolutions of the recoil telescope detectors were sufficient to distinguish recoiling boron ions with A=10 to 14. This isolation was necessary for the identification of transitions to bound states from those to states unbound against the emission of one or two neutrons. The recoil-detectors also shielded the downstream detector array from particles scattered from upstream collimation slits in the entrance beam-line of HELIOS. The silicon surface-barrier monitor telescope used to monitor the beam intensity was mounted on the recoil-detector assembly, on the downstream side. Figure 1 illustrates the experimental arrangement.

Figure 2 shows the kinematic relationship between the alpha-particle energy and position measured for events from ^{14}C (a) and ^{15}C (b) beams. Here, the kinematic group for each transition is an approximately straight line in the energy-versus-position plane. In Fig. 2(a) the groups corresponding to known 1^+, 2^+, and 3^+ levels in ^{12}B are indicated by the arrows. The data for the particle-bound 1^+ and 2^+ states, and those for the unbound 3^+ excitation, were obtained in coincidence with identified ^{12}B and ^{11}B nuclei, respectively. The few events for ^{11}B coincidences near z=1100 mm correspond to very shallow trajectories in the magnet whose energy-position correlations do not follow the diagonal lines for the strong excitations.

The data for the ^{15}C$(d,\alpha)^{13}$B appear in Fig. 2(b). The statistics are far reduced, however kinematic groups corresponding to bound and unbound excitations in ^{13}B are readily discerned. The star symbols represent events for transitions to particle-bound states in ^{13}B, and the red filled circles and green squares correspond to 1-n and 2-n unbound states, respectively. Events from the ground state and particle-bound excitations near 3.6 MeV can be seen. For alpha particles in coincidence with ^{12,11}B, several states are populated. For example, groups corresponding to excitation energies near 10.0 and 12 MeV are indicated by the dashed lines in Fig. 2(b). Note that for the excitations near 12 MeV both one- and two-neutron decays are present.

The same data are shown as Q-value spectra for the ^{14,15}C$(d,\alpha)^{12,13}$B reactions in Fig.3. The particle-bound excitations are shown in solid blue, and the events where the recoiling nucleus was unbound with respect to decay to either one, or two neutrons appear as the cross-hatched red, and green histograms, respectively. For ^{14}C$(d,\alpha)^{12}$B (Fig. 2(a)), transitions to the 1^+ and 2^+ ground and first-excited states are present, and weak evidence is found for the 2^+(3.782 MeV) and 1^+ (5.00 MeV) excitations. The resolution in excitation energy is approximately 240 keV FWHM, chiefly from a combination of target thickness and detector response. States at low excitation energy in ^{12}B with $J^\pi = 1^+$ or 2^+ can be formed from the $\pi(0p_{3/2})^{-1}\nu(0p_{1/2})$ or $\pi(0p_{3/2})^{-1}\nu(0p_{3/2})^{-1}$ configurations; the ground and first-excited states are predominantly the former, while the excited 1^+ and 2^+ states are mostly of the latter configuration. If the second 2^+ state is present, it must be through configuration mixing as here, $S=1$, $T=0$ pickup for pn pairs from the same orbital to even-spin states is forbidden. By far, the most strongly populated level is the known $3^+(\Gamma = 110\pm40$ keV) state at 5.61 MeV excitation, whose yield exceeds

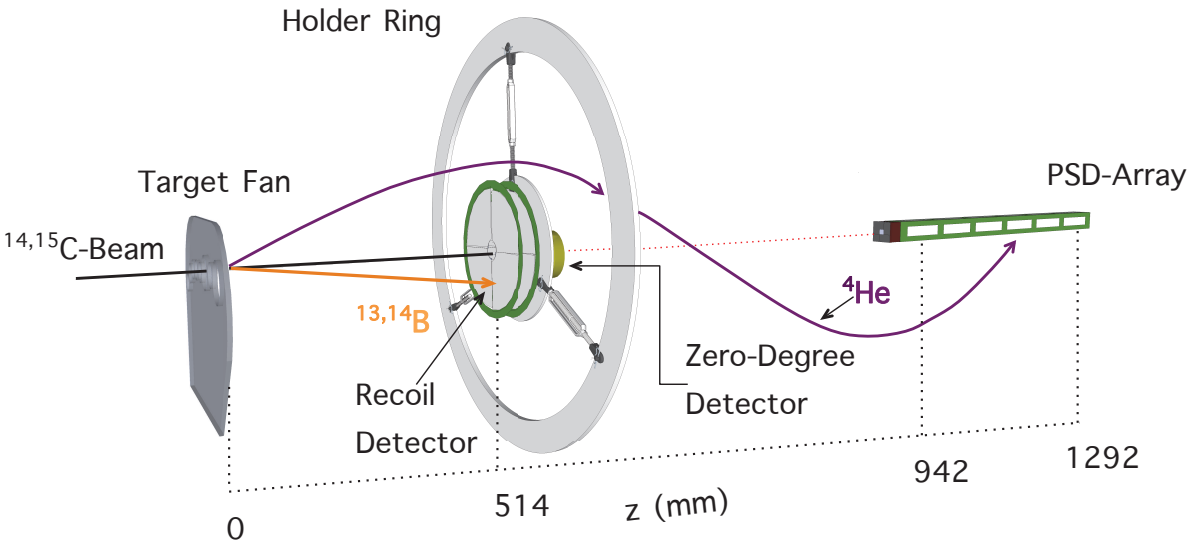

FIG. 1. (Color online) Schematic illustration of the HELIOS detector setup used to study ^{14,15}C$(d,\alpha)^{12,13}$B.

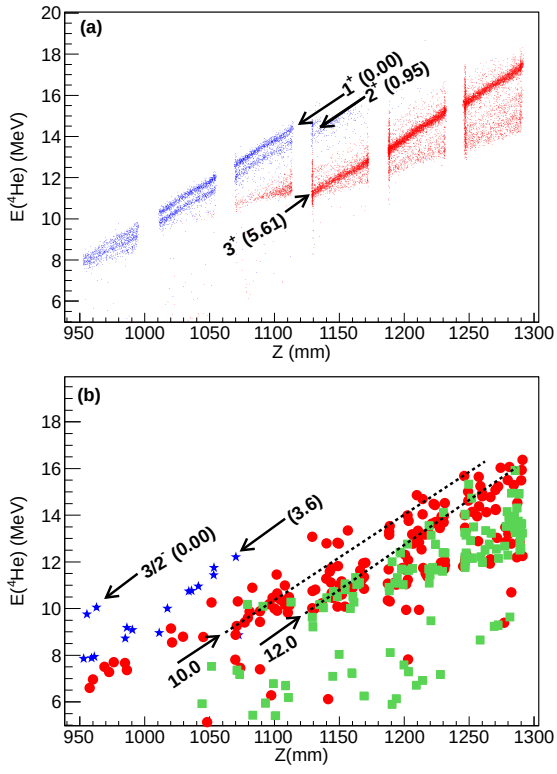

FIG. 2. (Color online) Kinematic relationship between alpha-particle energy and position in HELIOS, for the (a) ^{14}C$(d,\alpha)^{12}$B and (b) ^{15}C$(d,\alpha)^{13}$B reactions. In (a), the data in blue represent events obtained in coincidence with ^{12}B (blue) and ^{11}B (red). In (b), the (blue) stars, (red) filled circles and (green) filled squares represent alpha particles detected in coincidence with ^{13}B, ^{12}B, and ^{11}B, respectively. See text for details.

the combined yields of the ground and first-excited states by a factor of approximately 4, consistent with the favoring of the aligned configuration with $J = j_p + j_n$. The observed width of the state is $\Gamma \approx 350$ keV, presumably reflecting some contribution from the natural width of the state.

Data for the ^{15}C$(d,\alpha)^{13}$B reaction appear in Fig. 3(b,c). In the present geometry, the ^{13}B ground state is only barely on the edge of the acceptance as seen in Fig. 2(b). The ^{13}B $3/2^-$ ground state requires the removal of a $0p_{3/2}$ proton and $1s_{1/2}$ neutron and should not be populated strongly in this reaction. Weak transitions to bound states in ^{13}B near 3.6 MeV are also observed; $J^\pi = 1/2^+$ (3.48 MeV) and $5/2^+$ (3.68 MeV) have been found to be strongly populated by $\ell = 0$ and 2 transitions in the (d,p) reaction [14], $3/2^-$ (3.53 MeV) was identified in ^{7}Li(^{7}Li,p) [18], and $1/2^-$ (3.71 MeV) from ^{14}C$(d,^3$He) [19]. A number of states of unknown spin and parity are reported [20] in ^{13}B between E_X=5 to 11 MeV, however statistics and resolution preclude any firm association of these excitations to strength in this region in the present data. Given the reaction mechanism and the expected structures of the positive- and negative-parity states, it is likely that the most strongly populated states in the present work will be positive-parity $\pi(0p_{3/2}^{-1})\nu(0p_{1/2,3/2}^{-1}1s_{1/2})$ excitations. These configurations correspond to the same ones populated in ^{14}C$(d,\alpha)^{12}$B, with the additional $1s_{1/2}$ neutron acting as a spectator.

Figure 4 shows the ^{13}B data with one- and two-neutron unbound transitions combined, as well as the particle-bound states. The ^{12}B data are shown for comparison. The most prominent feature of the ^{13}B data is a possible doublet near $E_X(^{13}$B)=12 MeV. The strength of this feature in comparison to any other structure in

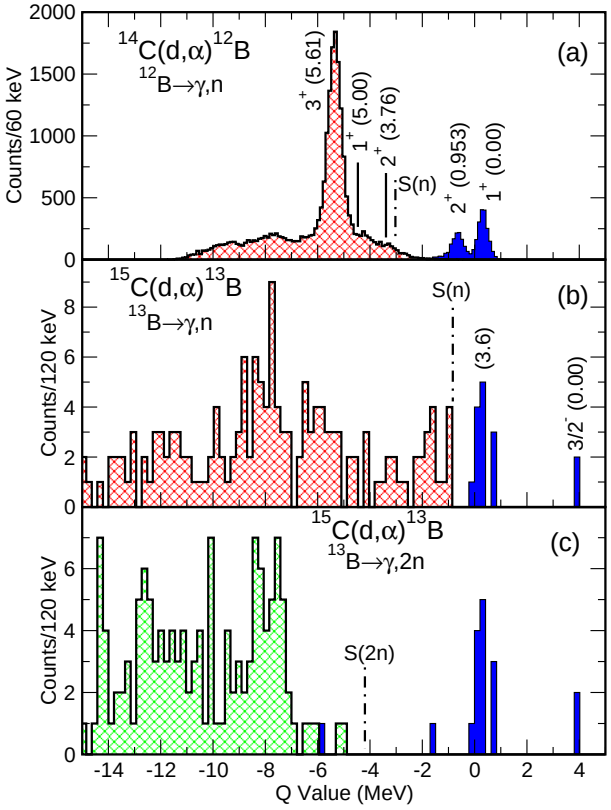

FIG. 3. (Color online) Q-value spectra for ^{14}C$(d,\alpha)^{12}$B (a) and ^{15}C$(d,\alpha)^{13}$B (b,c) reactions. The solid blue histograms represent transitions to particle bound states. The red and green cross-hatched histograms represent transitions to one-, and two-neutron unbound states, respectively.

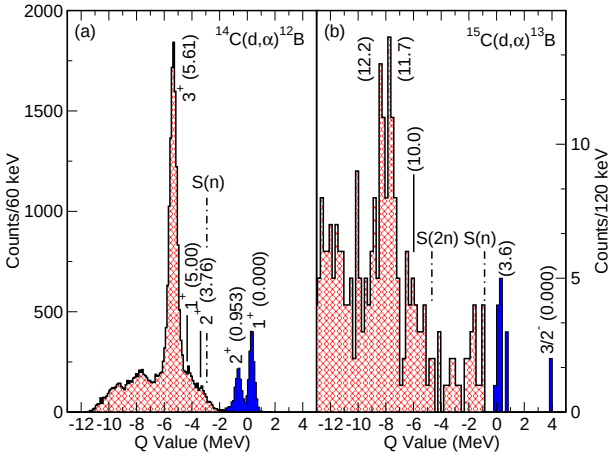

FIG. 4. (Color online) Q-value spectra for (a) ^{12}B from the ^{14}C$(d,\alpha)^{12}$B reaction, (b) ^{13}B from the ^{15}C$(d,\alpha)^{13}$B reaction. The solid histograms represent transitions to particle bound states. The red, cross-hatched histograms represent transitions to (a) neutron-unbound states in ^{12}B and (b) one- and two-neutron unbound states in ^{13}B.

the spectrum suggests that it arises from the coupling of the $[(0p_{3/2})^{-2}]_{3^+}$ state in ^{12}B to a valence $1s_{1/2}$ neutron, leading to excitations with $J^\pi = 5/2^+$ and $7/2^+$. The shift in Q-value for these states compared to the ^{12}B(3^+) level is qualitatively consistent with an expected monopole shift induced by the $s_{1/2}$ neutron interacting with the $p_{3/2}$ holes. Despite the fact that these states are nearly 4 MeV above the ^{13}B two-neutron decay threshold at S_{2n}=8.248 MeV, they appear to be relatively narrow and possess significant one-neutron decay branches as seen in Fig. 3(b). This observation is reasonable, since the favored decay of such excitations would be not only to the 3^+ state in ^{12}B, which is unbound to the emission of a second neutron, but also to the bound negative-parity doublet in ^{12}B at 1.67 and 2.62 MeV excitation energy that would not permit further neutron decay.

Further information about the nature of the strongly excited levels in the ^{13}B data may be found by examining the angular distributions, and comparing them to those obtained for transitions in the ^{14}C$(d,\alpha)^{12}$B reaction. Figure 5 shows angular distributions for the three strongest transitions in the ^{14}C$(d,\alpha)^{12}$B reaction, and the angular dependence of the summed yield for the two peaks of the structure at high excitation energy in ^{13}B. The angular distributions have been constructed from the measured yields, corrected for spectrometer acceptance and for the effects of recoil-coincidence efficiency. These effects have been analyzed using Monte-Carlo simulations of the transport properties of the spectrometer that include realistic detector geometries and the measured magnetic field (see Ref. [11] for more details). Where appropriate, the simulations treated the one- or two-neutron decay of the recoiling nuclei. Here, the angular distribution(s) of the emitted neutron(s) are assumed to be isotropic in the center-of-mass frame of the decaying nucleus. This assumption is not justified, however due to the strong focusing of the forward-going recoils and the acceptance of the recoil detector, neglect of any angular correlation does not affect the calculated detection efficiency.

In this case the ^{12}B(1^+) ground-state transition is expected to be dominantly ℓ=0, while the 2^+ and 3^+ states can only be populated with ℓ=2. The angular distributions for the three transitions are quite different from each other, as can be seen in Fig. 5. For the 1^+ (Fig. 5(a)) and 2^+ (Fig. 5(b)) states, the angular distributions show pronounced maxima, whereas the data for the 3^+ transition (Fig. 5(c), filled circles)are relatively featureless.

For comparison, the angular distribution measured for the 12 MeV structure in ^{13}B also appears in Fig. 5(c) (filled squares). The relative normalization here is arbitrary. The shape of the angular distribution is very similar to that of the 3^+ transition, as might be expected if these states were populated by the same pickup mechanism as that leading to the formation of the 3^+ state in ^{12}B. This similarity lends further support to the contention that this structure represents a doublet formed from the coupling of a $1s_{1/2}$ neutron to the aligned

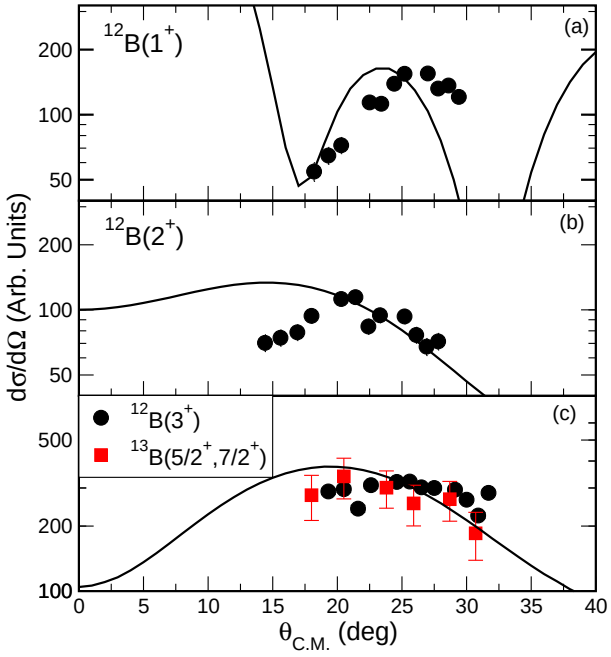

FIG. 5. (Color online) Angular-distribution data for different transitions to states in ^{12,13}B with the (d,α) reaction. The filled circles in (c) are data for the ^{12}B(3^+) excitation, and the filled squares for the suggested ^{13}B($5/2^+, 7/2^+$) doublet. The curves are qualitative indications of shapes that may be expected for single ℓ values: ℓ=0, 2, and 2 in (a), (b), and (c). The sample DWBA calculations are for transitions on ^{14}C at the appropriate Q values.

$[(0p_{3/2})^{-2}]_{3^+}$ configuration in ^{12}B.

The curves in Fig. 5 represent a calculation assuming a single-step direct pair transfer reaction performed using the code PTOLEMY. The deuteron optical-model parameters are the same as those used in [14, 15], and the alpha-particle parameters are from [6]. It is known that the angular distributions for two-nucleon transfer can be difficult to reproduce with distorted-wave Born approximation (DWBA) calculations [4, 6, 21]. These calculations are intended only to display qualitative indications of the approximate shapes to be expected from direct deuteron transfer with a single ℓ value. A 1^+ state can be populated by both ℓ=0 and 2 transitions and 3^+ by 2 and 4, while 2^+ must be ℓ=2. No attempt was made to obtain mixed transitions to better fit the data, nor to search optical-model parameters to obtain better fits. The ℓ=2 curves in Figs. 5 (b) and (c) are both for ^{14}C at the appropriate Q-values.

The angular distributions from the present data may be compared with those from the ^{16}O$(d,\alpha)^{14}$N reaction measured by van der Woude and de Meijer at E_d=20 MeV/nucleon [6]. In that case, the angular distribution for the 1^+ state at 3.95 MeV, which would correspond to the transition to the ^{12}B ground state, was fit dominantly by ℓ=0 transfer with a secondary maximum at an angle very similar to that for the peak in the ^{14}C$(d,\alpha)^{12}$B(1^+) angular distribution here. The 3^+ angular distributions

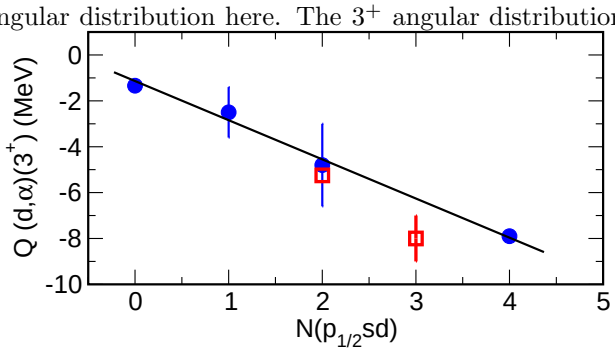

FIG. 6. (Color online) Dependence of the (d,α) Q value for the aligned 3^+ configuration on the number of nucleons beyond the $0p_{3/2}$ orbital ("N($p_{1/2}sd$)"). Points with error bars indicate that the strength is fragmented. The open symbols are the present results for ^{14,15}C. The line is to guide the eye.

for ^{14}N and ^{12}B are also very similar for similar angle ranges. The quality of the fits to the (d,α) data in Ref. [6] are no better in matching the data than the curves in Fig. 5, and indicate limitations of the models used for the reaction.

It is interesting to consider the dependence of the (d,α) reaction Q value for the 3^+ aligned state in p-shell nuclei on the number of nucleons beyond the $0p_{3/2}$ orbital. Figure 6 illustrates this dependence for ^{12,13}C, ^{14}N, and ^{16}O targets (filled symbols), as well as the results from the current measurement for ^{14,15}C (open symbols). For the nuclei with these nucleons in the $0p_{1/2}$ orbital, the Q value steadily decreases with increasing N($0p_{1/2}$). The result for ^{15}C departs from that systematic trend, likely due to the increased binding from the monopole interaction with the additional $1s_{1/2}$ neutron, as suggested above.

In summary, the observations of the strong 3^+ excitation in ^{12}B and a possible ($5/2^+$-$7/2^+$) doublet in ^{13}B populated by the (d,α) reaction are consistent with previous studies that showed the enhancement of aligned states populated with deuteron-transfer reactions. Due to the $T=0$ nature of the transferred pair, the properties of such states, for example their binding energies in more neutron-rich systems, can help inform our understanding of $T=0$ pairing and the monopole interaction in exotic nuclei. More systematic studies for such nuclei can provide additional data to guide shell-model and other calculations for such nuclei, and suggest that quasi-deuteron transfer with the (α,d) and (d,α) reactions can be useful tools, complementary to those currently used to study the structure of exotic nuclei.

This material is based upon work supported by the U. S. Department of Energy, Office of Science, Office of Nuclear Physics, under Award Numbers DE-FG02-04ER41320 and DE-AC02-06CH11357, and the U. S. National Science Foundation under Grant No. PHY-1068217. This research used resources of the Argonne National Laboratory ATLAS Accelerator Facility, which is a DOE Office of Science User Facility.

[1] Richard H. Pehl, Ernest Rivet, Joseph Cerny and Bernard G. Harvey, Phys. Rev. **137**, B114 (1965).
[2] Ernest Rivet, Richard H. Pehl, Joseph Cerny, and Bernard G. Harvey, Phys. Rev. **141**, 1021 (1966).
[3] C. C. Lu, M. S. Zisman, and B. G. Harvey, Phys. Rev. **186**, 1086 (1969).
[4] T. I. Bonner, Phys. Rev. C **1**, 1699 (1970).
[5] N. Frascaria, J. P. Didelez, J. P. Garron, E. Gerlic, and J. C. Roynette, Phys. Rev. C **10**, 1422 (1974).
[6] A. Van der Woude and R. J. de Meijer, Nucl. Phys. **A258**, 199 (1976).
[7] Norman K. Glendenning, Phys. Rev. **137**, B102 (1963).
[8] Norman K. Glendenning, Ann. Rev. of Nucl. Part. Sci. **13**, 191 (1963).
[9] S. Cohen and D. Kurath, Nucl. Phys. **A141**, 145 (1970).
[10] A. H. Wuosmaa *et al.,* Nucl. Instrum. and Meth. in Phys. Res. A **580**, 1290 (2007).
[11] J. C. Lighthall *et al.,* Nucl. Instrum. and Meth. in Phys. Res. A **622**, 97 (2010).
[12] B. Harss *et al.,* Rev. Sci. Instrum. **71**, 380 (2000).
[13] K. E. Rehm, J. Greene, B. Harss, D. Henderson, C. Jiang, R. C. Pardo, B. Zabransky, and M. Paul, Nucl. Instrum. in Phys. Res. A **647**, 3 (2011).
[14] B. B. Back *et al.,* Phys. Rev. Lett. **104**, 132501 (2010).
[15] A. H. Wuosmaa *et al.,* Phys. Rev. Lett. **105**, 132501 (2010).
[16] C. R. Hoffman *et al.,* Phys. Rev. C **85**, 054318 (2012).
[17] S. Bedoor *et al.*, Phys. Rev. C **88**, 011304R,(2013).
[18] H. Iwasaki *et al.*, Phys. Rev. Lett. **102**, 202502 (2009).
[19] G. Mairle and G. J. Wagner, Nucl. Phys. **A253**, 253 (1975).
[20] F. Azjenberg-Selove, Nucl. Phys. **A523**, 1 (1991).
[21] M. J. Schneider and W. W. Daehnick, Phys. Rev. C **4**, 1649 (1971).